New Energy-Preserving Finite Volume Element Scheme for the Korteweg-de Vries Equation

Jin-liang Yan and Liang-hong Zheng

***Abstract*—In this paper, an energy-preserving finite volume element scheme is proposed for the Korteweg-de Vries equation. The scheme is a combination of the discrete variational derivative method in time and the finite volume element method in space. The scheme can precisely conserve the global mass and energy at the discrete level, as well as has higher accuracy. For comparison, we also propose a momentum-preserving scheme and a finite volume element scheme. The numerical results demonstrate the remarkable accuracy and efficiency of our method compared with other schemes.**

***Index Terms*—Mass, Momentum, Energy, Finite volume element method, KdV equation.**

I. Introduction

THE ubiquitous Korteweg de-Dries (KdV) equation was first introduced by Boussinesq in 1877 and rediscovered by Korteweg and his Ph.D student de Vries [1] in 1895. The KdV equation models a variety of nonlinear phenomenona, such as shallow water waves, acoustic waves in a harmonic crystal and ion-acoustic waves in plasmas. The simplest form [2] of KdV equation is given by

$$u_t + \varepsilon u u_x + \mu u_{xxx} = 0,$$

where the function $u = u(x,t)$ represents the water's free surface in non-dimensional variable. The derivative u_t characterizes the time evolution of the wave propagating in one direction, the nonlinear term uu_x describes the steepening of the wave, and the linear term u_{xxx} accounts for the spreading or dispersion of the wave. In this paper we consider the following form of KdV equation:

$$u_t + \alpha u_x + \beta u u_x + \gamma u_{xxx} = 0, \quad a \le x \le b, \qquad (1)$$

where α, β, γ are constants given by

$$\alpha = c = \sqrt{gd}, \quad \beta = \frac{3c}{2d}, \quad \gamma = \frac{cd^2}{6}, \qquad (2)$$

with $c = \sqrt{gd}$, the shallow water speed. Here g is the gravitational acceleration and d is the average depth of water. The KdV equation is completely integrable [3] and give rise to multiple soliton solutions. The existence of conservation laws have been considered as an indiction of the integrability of the KdV. There is an infinite set of independent conservation laws for the KdV equation (1). The first three conservation laws of this set are:

$$M = \int_a^b u\,dx, \quad K = \frac{1}{2}\int_a^b u^2\,dx,$$
$$J = \int_a^b \left(\frac{\alpha}{2}u^2 + \frac{\beta}{6}u^3 - \frac{\gamma}{2}(u_x)^2\right)dx,$$

which correspond to mass, momentum and energy conservation law, respectively.

In this paper, the proposed energy-preserving scheme and momentum-preserving scheme are constructed using the discrete variational derivative method (DVDM) [4], which is a method of designing special numerical schemes that retain the conservation/dissipation properties of the original partial differential equations (PDEs). As to DVDM, researchers have done a lot of work, for example, Furihata and Mori [5] proposed a stable finite difference scheme for the Cahn-Hilliard equation. Koide and Furihata [6] designed four conservative schemes for the regularized long wave equation. Further, Matsuo and Furihata [7] extended the general studies to complex-valued PDEs, like the nonlinear Schrödinger equation. Recently, the method has been extended in various ways, for instance, Yaguchi, Matsuo and Sugihara [8] extended the method to nonuniform grids. Matsuo and Kuramae [9] proposed an alternating DVDM, and so on.

Finite volume element method (FVEM), as a type of important numerical tool for solving the differential equations, has a long history. This method is also known as a box method in some early references [10], or known as a generalized difference method [11] in China. The method has been widely used in several engineering fields, such as fluid mechanics, heat and mass transfer and petroleum engineering. Perhaps the most important property of FVEM is that it can preserve the conservation laws (mass, momentum and heat flux) on each computational cell. This important property, combined with adequate accuracy and ease of implementation, has attracted more people to do research in this field [12]–[15].

In this paper, we will propose an energy-preserving scheme for the KdV equation. The energy conservation law is an important property of the KdV equation. Thus, in the numerical simulation of the KdV equation, we hope retain this property. Moreover, to our knowledge, the energy-preserving scheme often has better stability, as well as smaller errors. Li and Vu-Quoc [16] once said that "in some areas, the ability to preserve some invariant properties of the original differential equation is a criterion to judge the success of a numerical simulation". Zhang [17] pointed out that the nonconservative schemes may easily show nonlinear blow-up. Thus, in view of this point, we hope design an energy-preserving scheme for the KdV equation (1). About the KdV equation, researchers have done a lot of work, for

Manuscript received December 02, 2016; revised March 24, 2017. This work was supported in part by the PhD Start-up Fund of Wuyi University (Grant No YJ201702), the Education Foundation of Fujian Province for Young Teachers (Grant No JA14319) and Undergraduate Technology Innovation Project of Fujian Province (Grant No SJ2011019).

Jin-Liang Yan is with the department of Mathematics and Computer, Wuyi University, Wuyi Shan, Fujian, 354300, China, e-mail: yanjinliang3333@163.com.

Liang-hong Zheng is with the department of Information and Computer Technology, No 1 middle school of Nanping, Nanping, Fujian, 353000, China. e-mail: 413845939@qq.com.

instance, Taha and Ablowitz [18] proposed a new scheme using the inverse scattering transform notion. Zhang and Wang [19] proposed an improved homogeneous balance method for Multi-Soliton Solutions of Gardner Equation. Ascher and McLachlan [20] developed and compared some symplectic and multi-symplectic finite difference schemes for the KdV equation. Bhatta and Bhatti [21] presented a new algorithm for approximating the numerical solution of the KdV equation in a modified B-polynomial basis. Darvishi, Kheybari and Khani [22] proposed a pseudospectral method for the KdV equation. Dağ and Dereli [23] developed a meshless method based on the radial basis functions. In this paper, we develop an energy-preserving scheme, and study their conservative properties, accuracy and long time behavior, and so on.

The organization of the paper is as follows. In Section 2, we present some notations and preliminaries about FVEM. In Section 3, we derive the proposed schemes, and analyze their conservative properties. In Section 4, we analyze the linear stability of the energy-preserving scheme. In Section 5, we present the numerical examples to illustrate the effectiveness of the new scheme. At last, we give some concise conclusions.

II. Notation and preliminaries

In this section, we define some notations and the framework of the FVEM.

First, we use a uniform grid T_h to discretize the solution domain, $a = x_0 < x_1 < x_2 < \cdots < x_{n-1} < x_n = b$ with grid spacing $h = x_i - x_{i-1} = (b-a)/n$. Then we place a dual grid T_h^*, $a = x_0 < x_{1/2} < x_{3/2} < \cdots < x_{n-1/2} < x_n = b$ with $x_{i-1/2} = (x_{i-1} + x_i)/2$, $i = 1, 2, \ldots, n$, and $I_0^* = [x_0, x_{1/2}]$, $I_i^* = [x_{i-1/2}, x_{i+1/2}]$ $(i = 1, 2, \ldots, n-1)$ and $I_N^* = [x_{N-1/2}, x_N]$ denote the dual elements.

The trial function space U_h is taken as the linear element space with respect to T_h. The basis function with respect to x_i is given by

$$\phi_i(x) = \begin{cases} 1 - h^{-1}|x - x_i|, & x_{i-1} \le x \le x_{i+1}, \\ 0, & \text{elsewhere.} \end{cases}$$

Thus, the functions $\{\phi_i(x) : i = 1, 2, \ldots, n\}$ form a basis of U_h and any $u_h \in U_h$ has the following expression

$$u_h = \sum_{i=1}^{N} u_i \phi_i(x),$$

where $u_i = u_h(x_i, t)$. Further, on the element I_i, we have

$$u_h = u_{i-1}(1 - \xi) + u_i \xi,$$

$$u_h^{'} = (u_i - u_{i-1})/h, \quad x \in I_i, \quad i = 1, 2, \ldots, n,$$

where $\xi = (x - x_{i-1})/h$.

Accordingly, the test function space V_h is chosen as the piecewise constant function (step function) space. The basis functions of V_h are

$$\psi_j(x) = \begin{cases} 1, & x_{j-1/2} \le x \le x_{j+1/2}, \\ 0, & \text{elsewhere,} \end{cases}$$

where $j = 1, 2, \ldots, n$.

Any $v_h \in V_h$ has the form

$$v_h = \sum_{i=1}^{N} v_i \psi_i(x),$$

where $v_i = v_h(x_i, t)$.

In the sequel, if not specially illustrate, we will use $U_k^{(m)}$ to denote the numerical solution at $x = x_k$ and $t = m\Delta t$, where Δt denotes the time step size. On the other hand, in this paper, we will adopt the following periodic boundary conditions,

$$\frac{\partial^j u}{\partial x^j}\Big|_{x=a} = \frac{\partial^j u}{\partial x^j}\Big|_{x=b} (j = 0, 1, 2). \tag{3}$$

III. Numerical schemes

In this section, we derive the proposed schemes and analyze their conservative properties.

A. Concrete form of the proposed scheme

For convenience, we define "free energy" or "local energy" of the KdV equation (1) as

$$G(u, u_x) = \frac{\alpha}{2}u^2 + \frac{\beta}{6}u^3 - \frac{\gamma}{2}(u_x)^2,$$

and its spatial integration

$$J(u) = \int_a^b G(u, u_x)\, dx$$

as the "global energy". Then Eq. (1) can be rewritten as

$$\frac{\partial u}{\partial t} = -\frac{\partial}{\partial x}\left(\frac{\delta G}{\delta u}\right), \tag{4}$$

where $\delta G/\delta u$ is the variational derivative of $G(u, u_x)$ defined by

$$\frac{\delta G}{\delta u} = \frac{\partial G}{\partial u} - \frac{\partial}{\partial x}\left(\frac{\partial G}{\partial u_x}\right).$$

In the following, we start to derive the proposed energy-preserving scheme. To this end, we first give a scheme of the "local energy"

$$\begin{aligned} G_{d,k}(U^{(m)}) &= \frac{\alpha}{2}(U_k^{(m)})^2 + \frac{\beta}{6}(U_k^{(m)})^3 \\ &- \frac{\gamma}{2}\frac{(\delta_k^+ U_k^{(m)})^2 + (\delta_k^- U_k^{(m)})^2}{2}, \end{aligned} \tag{5}$$

and the associated global energy is defined by

$$J_d(U^{(m)}) = \sum_{k=0}^{N}{}'' G_{d,k}(U^{(m)})\Delta x, \tag{6}$$

where

$$\sum_{k=0}^{N}{}'' g_k \triangleq \frac{1}{2}g_0 + g_1 + \cdots + g_{N-1} + \frac{1}{2}g_N.$$

By resorting to Eq. (5), a discrete scheme of the variational derivative corresponding to energy-preserving scheme is given by

$$\begin{aligned} \frac{\delta G_d}{\delta (U^{(m+1)}, U^{(m)})_k} &= \frac{\alpha}{2}(U_k^{(m+1)} + U_k^{(m)}) \\ &+ \frac{\beta}{6}\big((U_k^{(m+1)})^2 + U_k^{(m+1)}U_k^{(m)} + (U_k^{(m)})^2\big) \\ &+ \frac{\gamma}{2}\delta_k^{\langle 2\rangle}(U_k^{(m+1)} + U_k^{(m)}), \end{aligned} \tag{7}$$

where $\delta_k^{\langle 2\rangle}$ denotes the central difference quotient of $\partial^2/\partial x^2$. The above scheme is obtained by the following difference:

$$\begin{aligned}&\sum_{k=0}^{N}{}''\big(G_{d,k}(U^{(m+1)})-G_{d,k}(U^{(m)})\big)\Delta x\\&=\sum_{k=0}^{N}{}''\frac{\delta G_d}{\delta(U^{(m+1)},U^{(m)})_k}\big(U_k^{(m+1)}-U_k^{(m)}\big)\Delta x\\&+\text{boundary term.}\end{aligned}$$

The above method is also known as the discrete variational derivative method, more details about it please refer to [4]. After that we can obtain the fully discrete energy-preserving finite volume element scheme by substituting Eq. (7) into the following weak form

$$(\delta_m^+U^{(m)},\psi_i)=-\bigg(\frac{\partial}{\partial x}\bigg(\frac{\delta G_d}{\delta(U^{(m+1)},U^{(m)})}\bigg),\psi_i\bigg),\quad(8)$$

where $\delta_m^+U^{(m)}=(U^{(m+1)}-U^{(m)})/\Delta t$, Δt is the time step, $U^{(m)}\in U_h$ and $\psi_i\in V_h$ $(i=1,2,\ldots,N)$.

On the other hand, in order to reflect the superiority of the energy-preserving method, a momentum-preserving finite volume element scheme is also derived.

Let $(U_+^{(m+1/2)})_k\triangleq(U_{k+1}^{(m+1)}+U_{k+1}^{(m)})/2$, $(U_-^{(m+1/2)})_k\triangleq(U_{k-1}^{(m+1)}+U_{k-1}^{(m)})/2$, and substitute them into Eq. (7) and respectively in place of $U^{(m+1)}$ and $U^{(m)}$, then a discrete scheme of the variational derivative corresponding to the momentum-preserving scheme is obtained as follows

$$\begin{aligned}&\frac{\delta G_d}{\delta(U_+^{(m+1/2)},U_-^{(m+1/2)})_k}=\frac{\alpha}{2}\big((U_+^{(m+1/2)})_k+(U_-^{(m+1/2)})_k\big)\\&+\frac{\beta}{6}\big((U_+^{(m+1/2)})_k^2+(U_+^{(m+1/2)})_k(U_-^{(m+1/2)})_k\\&+(U_-^{(m+1/2)})_k^2\big)+\frac{\gamma}{2}\delta_k^{\langle 2\rangle}\big((U_+^{(m+1/2)})_k+(U_-^{(m+1/2)})_k\big).\end{aligned}$$

Substituting it into the following weak form

$$(\delta_m^+U^{(m)},\psi_j)=-\bigg(\frac{\partial}{\partial x}\bigg(\frac{\delta G_d}{\delta(U_+^{(m+1/2)},U_-^{(m+1/2)})}\bigg),\psi_j\bigg),\quad(9)$$

where $U^{(m)}\in U_h$ and $\psi_j\in V_h$ $(j=1,2,\ldots,N)$, we obtain the fully discrete momentum-preserving scheme.

At last, for comparison, we also derived the following implicit midpoint finite volume element scheme

$$\begin{aligned}&(\delta_m^+U^{(m)},\psi_k)=\beta\big(U^{(m+1/2)}U_x^{(m+1/2)},\psi_k\big)\\&-\alpha\big(U_x^{(m+1/2)},\psi_k\big)+\gamma\big(U_{xxx}^{(m+1/2)},\psi_k\big),\end{aligned}\quad(10)$$

where $U^{(m+1/2)}=(U^{(m+1)}+U^{(m)})/2$, $U^{(m)}\in U_h$, and $\psi_k\in V_h$ $(k=1,2,\ldots,N)$.

In addition, in order to illustrate the conservative properties of the schemes (9) and (10), we also consider the following discrete quantities, i.e., the global mass and the global momentum

$$\begin{aligned}M_d(U^{(m)})&=\sum_{k=0}^{N}{}''U_k^{(m)}\Delta x,\\K_d(U^{(m)})&=\frac{1}{2}\sum_{k=0}^{N}{}''(U_k^{(m)})^2\Delta x.\end{aligned}\quad(11)$$

B. Conservation properties of the proposed schemes

In the following, we start to study the conservative properties of the KdV equation (1).

Proposition III.1. *Let u be the analytical solution of (4), and assume the following boundary condition*

$$-\bigg[\frac{\delta G}{\delta u}\bigg]_{x=a}^{b}=0$$

is satisfied, then the continuous mass M is constant, that is

$$\frac{d}{dt}\int_a^b u\,dx=0.$$

Proof:

$$\begin{aligned}&\frac{d}{dt}\int_a^b u\,dx=\int_a^b u_t\,dx\\&=-\int_a^b\frac{\partial}{\partial x}\bigg(\frac{\delta G}{\delta u}\bigg)\,dx=-\bigg[\frac{\delta G}{\delta u}\bigg]_{x=a}^{b}=0.\end{aligned}$$

■

Proposition III.2. *Let u be the analytical solution of (4), and assume the following boundary conditions*

$$-\bigg[u\frac{\delta G}{\delta u}\bigg]_{x=a}^{b}=0,\quad\big[G(u,u_x)\big]_{x=a}^{b}=0$$

are satisfied, then the continuous momentum K is constant, that is

$$\frac{1}{2}\frac{d}{dt}\int_a^b u^2\,dx=0.$$

Proof:

$$\begin{aligned}&\frac{1}{2}\frac{d}{dt}\int_a^b u^2\,dx=\int_a^b uu_t\,dx\\&=-\int_a^b u\frac{\partial}{\partial x}\bigg(\frac{\delta G}{\delta u}\bigg)\,dx\\&=-\bigg[u\frac{\delta G}{\delta u}\bigg]_{x=a}^{b}+\int_a^b\frac{\partial u}{\partial x}\frac{\delta G}{\delta u}\,dx\\&=\int_a^b\frac{\partial}{\partial x}G(u,u_x)\,dx=\big[G(u,u_x)\big]_{x=a}^{b}=0.\end{aligned}$$

■

Proposition III.3. *Let u be the analytical solution of (4), and assume the following boundary conditions*

$$\bigg[\frac{\partial G}{\partial u_x}\frac{\partial u}{\partial t}\bigg]_{x=a}^{b}=0,\quad\bigg[-\frac{1}{2}\Big(\frac{\delta G}{\delta u}\Big)^2\bigg]_{x=a}^{b}=0$$

are satisfied, then the continuous energy J is constant, that is

$$\frac{d}{dt}\int_a^b G(u,u_x)\,dx=0.$$

Proof:

$$\begin{aligned}
&\frac{d}{dt}\int_a^b G(u,u_x)\,dx = \int_a^b \frac{\partial G}{\partial t}\,dx \\
&= \int_a^b \left(\frac{\partial G}{\partial u}\frac{\partial u}{\partial t} + \frac{\partial G}{\partial u_x}\frac{\partial u_x}{\partial t}\right) dx \\
&= \int_a^b \frac{\partial G}{\partial u}\frac{\partial u}{\partial t}\,dx - \int_a^b \frac{\partial u}{\partial t}\frac{\partial}{\partial x}\left(\frac{\partial G}{\partial u_x}\right) dx \\
&= \int_a^b \frac{\delta G}{\delta u}\frac{\partial u}{\partial t}\,dx = -\int_a^b \frac{\delta G}{\delta u}\frac{\partial}{\partial x}\left(\frac{\delta G}{\delta u}\right) dx \\
&= -\frac{1}{2}\int_a^b \frac{\partial}{\partial x}\left(\frac{\delta G}{\delta u}\right)^2 dx = \left[-\frac{1}{2}\left(\frac{\delta G}{\delta u}\right)^2\right]_{x=a}^{b} = 0.
\end{aligned}$$

■

Similarly we have the following conservative properties.

Theorem III.1. *(Discrete mass conservation law) Let $U = U^{(m)}$ be the solution of (8), and assume the following boundary condition*

$$\left[\frac{\delta G_d}{\delta(U^{(m+1)}, U^{(m)})}\right]_{x=a}^{b} = 0$$

is satisfied, then the discrete mass M_d is constant, namely

$$\int_a^b U^{(m)}\,dx = const.$$

Proof:

$$\begin{aligned}
&\frac{1}{\Delta t}\int_a^b \left(U^{(m+1)} - U^{(m)}\right) dx \\
&= \int_a^b \left(\frac{U^{(m+1)} - U^{(m)}}{\Delta t}\right) dx \\
&= -\int_a^b \frac{\partial}{\partial x}\left(\frac{\delta G_d}{\delta(U^{(m+1)}, U^{(m)})}\right) dx \\
&= \left[-\frac{\delta G_d}{\delta(U^{(m+1)}, U^{(m)})}\right]_{x=a}^{b} = 0.
\end{aligned}$$

■

Theorem III.2. *(Discrete energy conservation law) Let $U = U^{(m)}$ be the solution of (8), and assume the following boundary condition*

$$\left[-\frac{1}{2}\left(\frac{\delta G_d}{\delta(U^{(m+1)}, U^{(m)})}\right)^2\right]_{x=a}^{b} = 0$$

is satisfied, then the discrete energy J_d is constant, namely

$$\int_a^b G_d(U^{(m)})\,dx = const.$$

Proof:

$$\begin{aligned}
&\frac{1}{\Delta t}\int_a^b \left(G_d(U^{(m+1)}) - G_d(U^{(m)})\right) dx \\
&= \int_a^b \frac{\delta G_d}{\delta(U^{(m+1)}, U^{(m)})}\left(\frac{U^{(m+1)} - U^{(m)}}{\Delta t}\right) dx \\
&= -\int_a^b \frac{\delta G_d}{\delta(U^{(m+1)}, U^{(m)})}\frac{\partial}{\partial x}\left(\frac{\delta G_d}{\delta(U^{(m+1)}, U^{(m)})}\right) dx \\
&= -\frac{1}{2}\int_a^b \frac{\partial}{\partial x}\left(\frac{\delta G_d}{\delta(U^{(m+1)}, U^{(m)})}\right)^2 dx \\
&= \left[-\frac{1}{2}\left(\frac{\delta G_d}{\delta(U^{(m+1)}, U^{(m)})}\right)^2\right]_{x=a}^{b} = 0.
\end{aligned}$$

■

Theorem III.3. *(Discrete mass conservation law) Let $U = U^{(m)}$ be the solution of (9), and assume the following boundary condition*

$$\left[\frac{\delta G_d}{\delta(U_+^{(m)}, U_-^{(m)})}\right]_{x=a}^{b} = 0$$

is satisfied, then the discrete mass M_d is constant, namely

$$\int_a^b U^{(m)}\,dx = const.$$

Proof:

$$\begin{aligned}
&\frac{1}{\Delta t}\int_a^b \left(U^{(m+1)} - U^{(m)}\right) dx \\
&= \int_a^b \left(\frac{U^{(m+1)} - U^{(m)}}{\Delta t}\right) dx \\
&= -\int_a^b \frac{\partial}{\partial x}\left(\frac{\delta G_d}{\delta(U_+^{(m)}, U_-^{(m)})}\right) dx \\
&= \left[-\frac{\delta G_d}{\delta(U_+^{(m)}, U_-^{(m)})}\right]_{x=a}^{b} = 0.
\end{aligned}$$

■

Theorem III.4. *(Discrete momentum conservation law) Let $U = U^{(m)}$ be the solution of (9), and assume the following boundary conditions*

$$\left[\frac{U^{(m+1)} + U^{(m)}}{2}\frac{\delta G_d}{\delta(U_+^{(m)}, U_-^{(m)})}\right]_{x=a}^{b} = 0$$
$$\left[G_d(U^{(m)}, U^{(m+1)})\right]_{x=a}^{b} = 0$$

are satisfied, then the discrete momentum K_d is constant, namely

$$\frac{1}{2}\int_a^b (U^{(m)})^2\,dx = const.$$

Proof:

$$\begin{aligned}
&\frac{1}{2\Delta t}\int_a^b \left[(U^{(m+1)})^2-(U^{(m)})^2\right]dx\\
&=\int_a^b\left(\frac{U^{(m+1)}+U^{(m)}}{2}\right)\left(\frac{U^{(m+1)}-U^{(m)}}{\Delta t}\right)dx\\
&=\int_a^b\left(\frac{U^{(m+1)}+U^{(m)}}{2}\right)\delta_m^+U^{(m)}dx\\
&=-\int_a^b\left(\frac{U^{(m+1)}+U^{(m)}}{2}\right)\frac{\partial}{\partial x}\left(\frac{\delta G_d}{\delta(U_+^{(m)},U_-^{(m)})}\right)dx\\
&=\int_a^b\frac{\partial}{\partial x}\left(\frac{U^{(m+1)}+U^{(m)}}{2}\right)\frac{\delta G_d}{\delta(U_+^{(m)},U_-^{(m)})}\,dx\\
&=\int_a^b\frac{\partial}{\partial x}G_d(U^{(m)},U^{(m+1)})\,dx\\
&=\left[G_d(U^{(m)},U^{(m+1)})\right]_{x=a}^b=0.
\end{aligned}$$

■

In the above equations, integration by parts formula and periodic boundary conditions are used. At last, for the standard finite volume element scheme (10), we also have the following conservative property, namely

Theorem III.5. *(Discrete mass conservation law.) Let $U=(U_k)_{k\in\mathbf{Z}}$ be the solution of (10), then the discrete mass M_d is constant, namely*

$$\int_a^b U^{(m)}dx=const.$$

The proof of Theorem III.5 is similar to the one of Theorem III.1.

IV. Stability analysis

In this section, we study the stability of the energy-preserving scheme (8) for solving Eq. (1). Here we only consider equations without nonlinear terms, which allow us to study the linear stability of the proposed schemes using the Fourier method.

Firstly, from Eq. (8), we get the following fully discrete energy-preserving scheme:

$$\begin{aligned}
&\alpha_1U_{k-2}^{(m+1)}+\alpha_2U_{k-1}^{(m+1)}+\alpha_3U_k^{(m+1)}-\alpha_2U_{k+1}^{(m+1)}\\
&-\alpha_1U_{k+2}^{(m+1)}=-\alpha_1U_{k-2}^{(m)}-\alpha_2U_{k-1}^{(m)}+\alpha_3U_k^{(m)}\\
&+\alpha_2U_{k+1}^{(m)}+\alpha_1U_{k+2}^{(m)}\\
&+\alpha_4\big[\big((U_{k-1}^{(m+1)})^2+U_{k-1}^{(m+1)}U_{k-1}^{(m)}+(U_{k-1}^{(m)})^2\big)\\
&-\big((U_{k+1}^{(m+1)})^2+U_{k+1}^{(m+1)}U_{k+1}^{(m)}+(U_{k+1}^{(m)})^2\big)\big],
\end{aligned}\tag{12}$$

where $j=0,1,\ldots,N$,

$$\begin{aligned}
&\alpha_1=-\gamma\Delta t,\alpha_2=6\gamma\Delta t-3\alpha h^2\Delta t,\\
&\alpha_3=12h^3,\alpha_4=\beta h^2\Delta t.
\end{aligned}$$

For the linear Fourier analysis, we only consider the linear version of Eq. (12), which is given by

$$\begin{aligned}
&\alpha_1U_{k-2}^{(m+1)}+\alpha_2U_{k-1}^{(m+1)}+\alpha_3U_k^{(m+1)}-\alpha_2U_{k+1}^{(m+1)}\\
&-\alpha_1U_{k+2}^{(m+1)}=-\alpha_1U_{k-2}^{(m)}-\alpha_2U_{k-1}^{(m)}+\alpha_3U_k^{(m)}\\
&+\alpha_2U_{k+1}^{(m)}+\alpha_1U_{k+2}^{(m)}.
\end{aligned}\tag{13}$$

Then assume that $U_j^{(m)}$ is periodic in x-direction, and at grid node x_j, let

$$U_j^{(m)}=V^{(m)}e^{i\omega jh},\tag{14}$$

where $V^{(m)}$ is amplitude at time level m, and ω is phase angle in x-direction. Substituting (14) into (13), we have

$$(\alpha_3-i\alpha_5)V^{(m+1)}=(\alpha_3+i\alpha_5)V^{(m)},$$

where

$$\alpha_5=2\alpha_1\sin(2wh)+2\alpha_2\sin(wh).$$

Therefore, the growth factor g for the proposed energy-preserving scheme is

$$|g|=\left|\frac{V^{(m+1)}}{V^{(m)}}\right|=\left|\frac{\alpha_3+i\alpha_5}{\alpha_3-i\alpha_5}\right|=1.$$

Therefore, it meets the unconditionally stable criterion ($|g|\le 1$) and we conclude that the proposed energy-preserving scheme is unconditionally stable.

V. Numerical experiments

In this section, we will test the proposed schemes numerically. Through these numerical examples, we will analyze the accuracy and conservative properties of the proposed schemes, and further illustrate the advantages of the energy-preserving scheme.

A. Single solitary wave

Here we consider the KdV equation (1), and set $A=1$, $d=6$ and $g=9.8$, then we can obtain α, c, β and γ by (2). According to [21], Eq. (1) has the following solitary wave solution:

$$u(x,t)=A\ \mathrm{sech}^2\left[\frac{1}{2}\sqrt{\frac{3A}{d^3}}(x-\kappa t)\right],$$

where $\kappa=c\big(1+\frac{A}{2d}\big)$. This solution corresponds to a solitary wave of amplitude A. Here c denotes the velocity of the traveling wave. Here we adopt the following initial solution

$$u(x,0)=A\ \mathrm{sech}^2\left[\frac{1}{2}\sqrt{\frac{3A}{d^3}}x\right],$$

and the periodic boundary condition

$$u(a,t)=u(b,t).$$

On the other hand, in order to validate the efficiency of the proposed methods, in the sequel, we will use $L_\infty=\max_{0\le i\le N-1}|U(x_i,t_n)-u_i^{(n)}|$ and order $=\log_2\big(\|u^n-U_{2h}^{(n)}\|_\infty/\|u^{(n)}-U_h^{(n)}\|_\infty\big)$ to evaluate the accuracy and the convergence orders of the methods. In addition, we will use $|I_i^n-I_i^1|/I_i^1$ to denote the relative errors of the invariants, where $I_i(i=1,2,3)$ respectively corresponds to the global energy (6) and mass, momentum (11) at the discrete level.

Firstly, we test the accuracy and the convergence orders of the proposed schemes. Here we assume the problem is solved on the interval $[-100,100]$. In order to measure the error in space, a relatively small time step $\Delta t=0.0001$ is chosen such that the error from the time direction can be negligible, and the spatial steps are respectively chosen as $h=2$, $h=1$, $h=1/2$ and $h=1/4$. The spatial L_∞ errors and corresponding convergence rates of the proposed

TABLE I: Spatial L_∞ errors and convergence orders of the proposed methods with $N = 1000$, $\Delta t = 0.0001$, $-100 \le x \le 100$.

h	MFVEM	order	EFVEM	order	FVEM	order
2	$1.6914e-03$	—	$4.0981e-04$	—	$4.0981e-04$	—
1	$4.3487e-04$	1.96	$1.0390e-04$	1.98	$1.0390e-04$	1.98
$1/2$	$1.0934e-04$	1.99	$2.5993e-05$	2.00	$2.5993e-05$	2.00
$1/4$	$2.7368e-05$	2.00	$6.5672e-06$	1.98	$6.5672e-06$	1.98

TABLE II: Temporal L_∞ errors and convergence orders of the proposed methods with $T = 1$, $h = 1/16$, $-100 \le x \le 100$.

Δt	MFVEM	order	EFVEM	order	FVEM	order
$1/2$	$8.7962e-03$	—	$9.1200e-03$	—	$8.7841e-03$	—
$1/4$	$2.3166e-03$	1.92	$2.3943e-03$	1.93	$2.3035e-03$	1.93
$1/8$	$5.9953e-04$	1.95	$6.0927e-04$	1.97	$5.8609e-04$	1.97
$1/16$	$1.6364e-04$	1.87	$1.5595e-04$	1.97	$1.5012e-04$	1.97

TABLE III: L_∞ errors and convergence orders of the proposed methods with $T = 3$, $h = \Delta t$, $-100 \le x \le 100$.

h	MFVEM	order	EFVEM	order	FVEM	order
1	$9.7275e-02$	—	$9.2927e-02$	—	$9.0518e-02$	—
$1/2$	$2.9056e-02$	1.74	$2.7584e-02$	1.75	$2.6806e-02$	1.76
$1/4$	$7.657e-03$	1.92	$7.2513e-03$	1.93	$7.0406e-03$	1.93
$1/8$	$1.9412e-03$	1.98	$1.8372e-03$	1.98	$1.7833e-03$	1.98

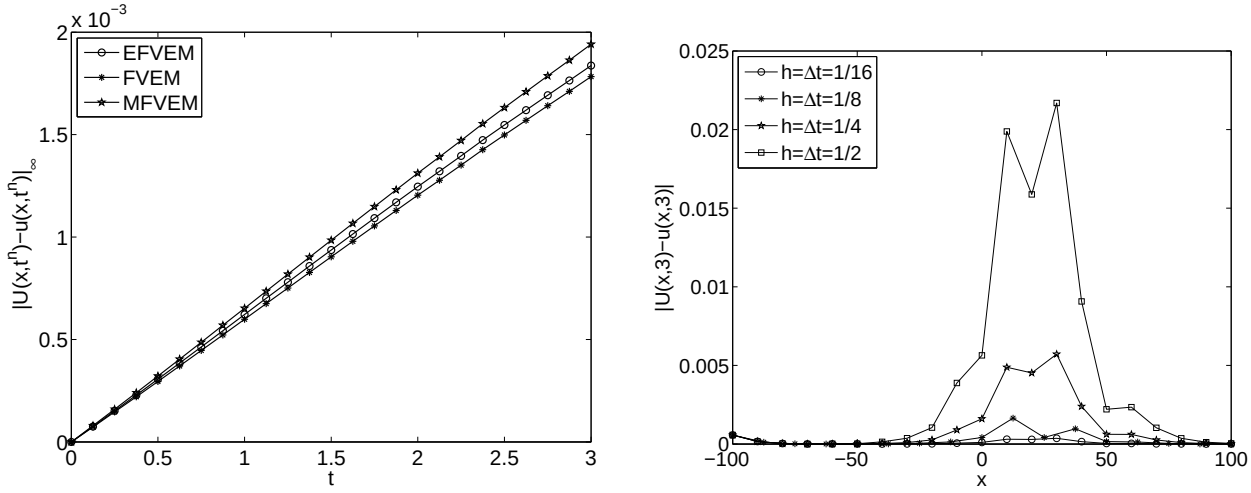

(a) (b)

Fig. 1: The errors of the proposed schemes: (a) the maximum errors of the three proposed schemes at $T = 3$ and with $h = \Delta t = 1/16$, (b) the numerical errors corresponding to different steps of the energy-preserving scheme at $T = 3$.

methods are presented in Table I, which clearly shows that the energy-preserving scheme and the finite volume element scheme have higher accuracy than the momentum-preserving scheme. Similarly, for the time direction, a relatively small spatial step $h = 1/16$ is chosen such that the error from the spatial direction can be negligible. The temporal L_∞ error and corresponding convergence rates of the proposed methods are presented in Table II, which clearly shows that the convergence rates of three methods are approximately equal to 2. It is also noted that the error of the momentum-preserving scheme cease to decrease at a certain point, which is because the error from the time direction become very small such that it can not be distinguished from the spatial error. On the other hand, the L_∞ errors and the convergence rates of three methods with $h = \Delta t$ and $T = 3$ are presented in Table III, which clearly shows that the convergence rates of three methods are all approximately equal to 2 in space and time.

Secondly, in order to compare the accuracy of the proposed methods, we plot the variation of the L_∞ errors of the proposed methods, when $h = \Delta t = 1/16$ and $T = 3$, in Figure 1(a), which clearly shows that the growth of the errors of three methods are linear, and the momentum-preserving scheme has the largest error. On the other hand, Figure 1(b) presents the numerical errors corresponding to different steps of the energy-preserving scheme at $T = 3$.

At last, we test the propagation of the solitary wave and the conservative properties of the proposed schemes. In the sequel, we set spatial step $h = 0.5$ and temporal step $\Delta t = 0.1$, and the problem is solved over the interval $[-50, 50]$. Figure 2 presents the numerical results of the energy-preserving scheme for t in $[0, 40]$. The surface plot

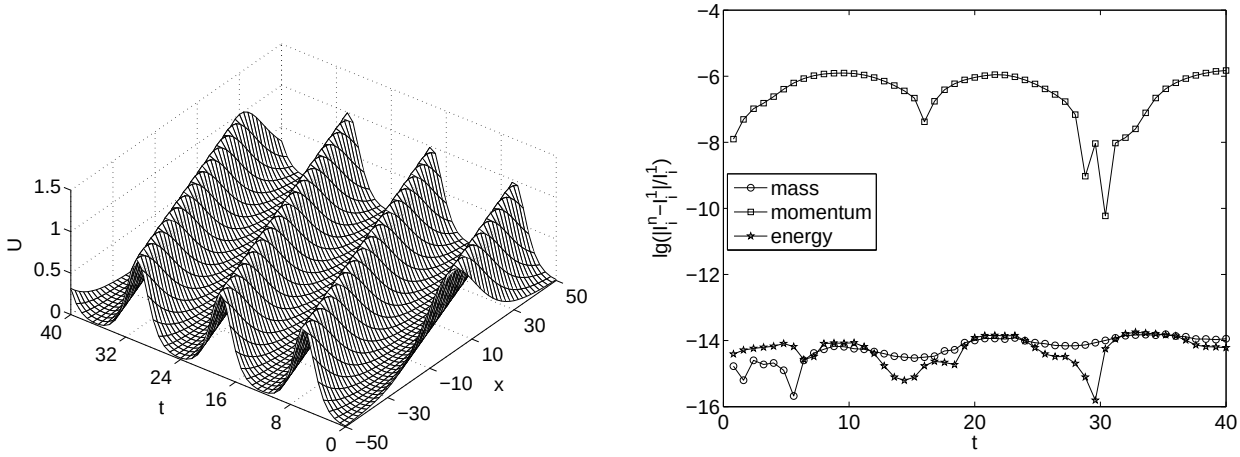

(a) (b)

Fig. 2: The numerical results of the energy-preserving scheme: (a) numerical solution, (b) the relative errors of invariants, when $h = 0.5$, $\Delta t = 0.1$, $a = 1$, $d = 6$, $T = 40$ and $-50 \leq x \leq 50$.

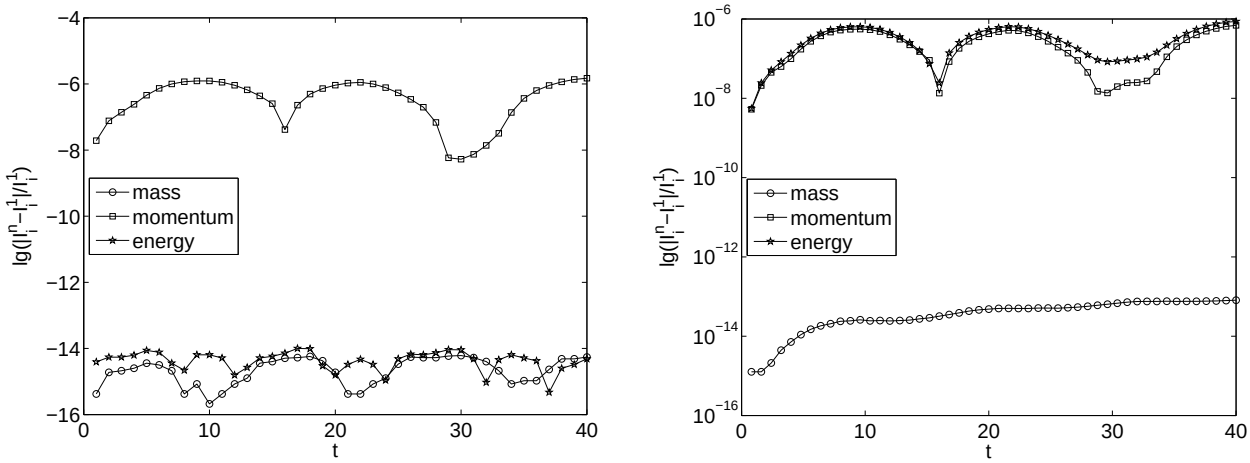

(a) (b)

Fig. 3: The relative errors of the invariants of the proposed schemes: (a) momentum-preserving scheme, (b) finite volume element scheme, when $h = 0.5$, $\Delta t = 0.1$, $a = 1$, $d = 6$, $T = 40$ and $-50 \leq x \leq 50$.

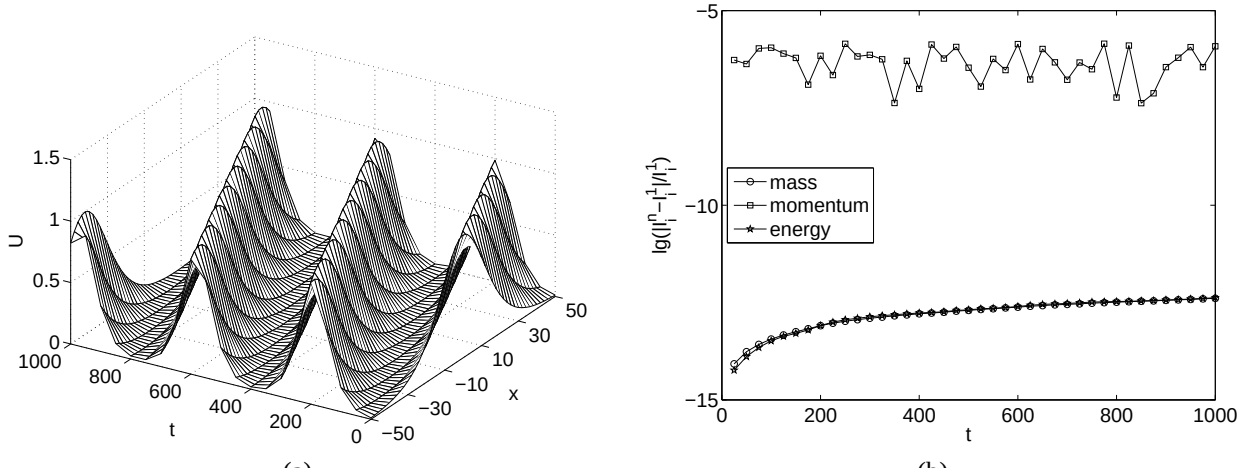

(a) (b)

Fig. 4: The numerical results of the energy-preserving scheme: (a) numerical solution, (b) the relative errors of invariants, when $h = 0.5$, $\Delta t = 0.1$, $a = 1$, $d = 6$, $T = 1000$ and $-50 \leq x \leq 50$.

of numerical solution at time $T = 40$ is presented in Figure 2(a), which shows the solitary wave moves to the right at a constant speed, and the wave shape and amplitude almost unchanged with time increase. Figure 2(b) shows that the relative errors of the invariants at the discrete level. It is clearly seen that the energy-preserving method can

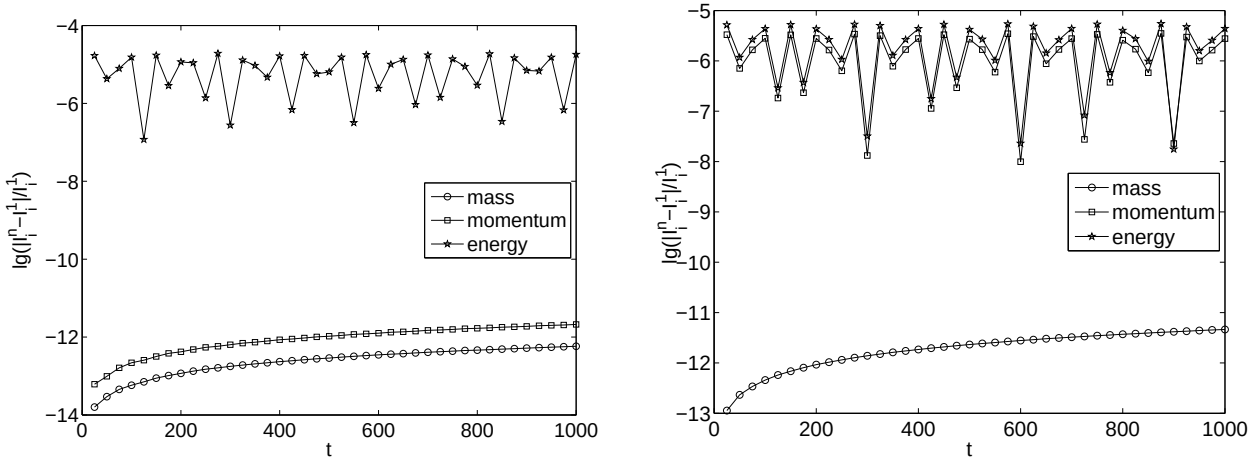

(a) (b)

Fig. 5: The relative errors of the invariants of the proposed schemes: (a) momentum-preserving scheme, (b) finite volume element scheme, when $h = 0.5$, $\Delta t = 0.1$, $a = 1$, $d = 6$, $T = 1000$ and $-50 \leq x \leq 50$.

precisely preserve the discrete mass and energy to within machine precision. The relative errors of the invariants of the momentum-preserving scheme and the finite volume element scheme are presented in Figure 3, which shows that the momentum-preserving scheme can precisely conserve the discrete mass and momentum to within machine precision, and the finite volume element scheme can precisely conserve the discrete mass to within machine precision. In view of Figure 2 and Figure 3, we conclude that three schemes all can be used to simulate the propagation of the solitary wave, but in the aspect of accuracy and conservation properties, the energy-preserving method is a better method. On the other hand, in order to test the long time behavior of the energy-preserving scheme, we also present the numerical results of the energy-preserving method for t in $[0, 1000]$ in Figure 4, which illustrates the scheme has good stability and long time computation ability. In addition, for comparison, we also present the relative errors of the invariants of the momentum-preserving scheme and the finite volume element scheme in Figure 5.

B. Interaction of two solitary waves

In order to further illustrate the effectiveness of the proposed scheme, here we discuss the interaction of two solitary waves. Setting $\alpha = 0$, $\beta = 1$, $\gamma = 4.84 \times 10^{-4}$, then we obtain the following KdV equation,

$$u_t + uu_x + 4.84 \times 10^{-4} u_{xxx} = 0, \quad 0 \leq x \leq 4. \tag{15}$$

Here we consider the KdV equation (15) with the following periodic boundary condition

$$u(0, t) = u(4, t), \quad t > 0.$$

On the other hand, according to [18], [24], Eq. (15) has the following exact solution,

$$u(x, t) = 12\gamma(\log F)_{xx}, \tag{16}$$

where

$$F = 1 + \exp(\eta_1) + \exp(\eta_2) + \left(\frac{l_1 - l_2}{l_1 + l_2}\right)^2 \exp(\eta_1 + \eta_2),$$
$$\eta_i = l_i x - l_i^3 \gamma t + m_i (i = 1, 2),$$
$$l_1 = \sqrt{\frac{0.3}{\gamma}}, \quad l_2 = \sqrt{\frac{0.1}{\gamma}}, \quad m_1 = -0.48 l_1, \quad m_2 = -1.07 l_2.$$

For all the computations, we have used the stepsizes $h = 0.0125$, $\Delta t = 0.05$, and the computations are done up to time $T = 6$. The numerical results of the energy-preserving scheme are presented in Figure 6, which shows that the energy-preserving scheme can exactly preserve the global mass and energy at the discrete level. On the other hand, Figures 7-9 display the interaction process of two solitary waves. It is noted that the taller wave initially located on the left of the lower wave. Then, at $t = 2.5$, the taller wave catched up the lower wave and occurred interaction, and at $t = 3$ and $t = 3.5$, the taller wave and the lower wave overlapped, as is noted in Figure 8. It is also noted that the taller wave and the lower wave started to leave away when $t > 3.5$, and the taller wave and the lower wave interchanged their positions at $t = 6$, as is shown in Figure 9. On the other hand, the numerical results also shows that the energy-preserving scheme has better performances than the ones of [24], i.e., the method of [24] needs smaller stepsizes and is not suitable for long time computation.

VI. Conclusions

In this paper, an energy-preserving scheme is proposed for the Korteweg-de Vries equation. We investigate the accuracy and the conservative properties of the proposed method and compare its performances with the ones of a momentum-preserving scheme and a finite volume element scheme. The numerical results show that three schemes all can simulate the KdV equation, but in the aspect of accuracy and conservative properties, the energy-preserving scheme has smaller accuracy and better conservative properties than other two schemes. Thus the energy-preserving scheme is a better choice for the KdV equation. Besides, the energy-preserving scheme is unconditionally stable and has better long time computation ability.

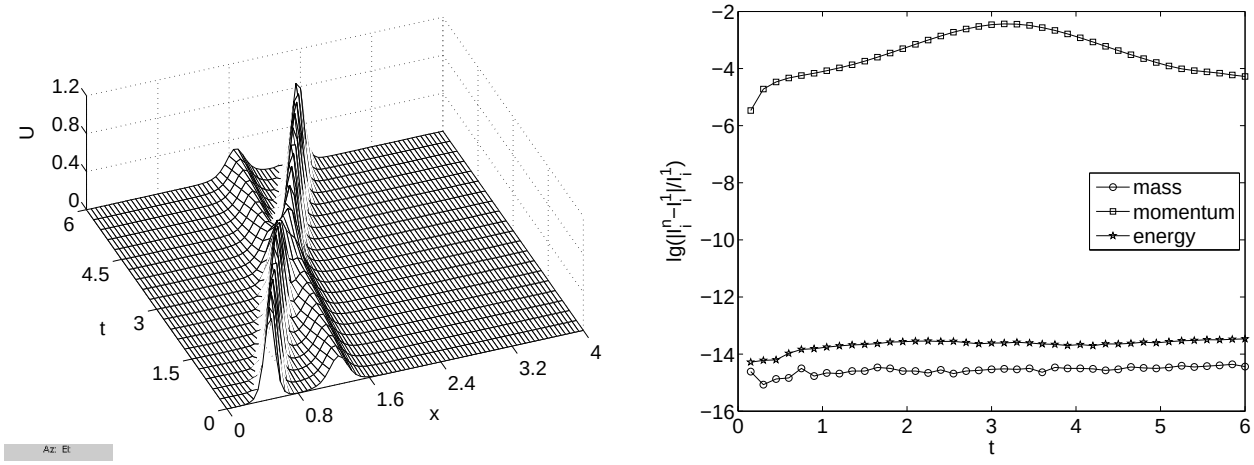

(a) (b)

Fig. 6: The numerical results of the two solitary waves obtained by the energy-preserving scheme: (a) the surface plot of numerical solution, (b) the relative errors of invariants, when $\alpha = 0$, $\beta = 1$, $\mu = 4.84 \times 10^{-4}$, $h = 0.0125$, $T = 6$, and $0 \leq x \leq 4$.

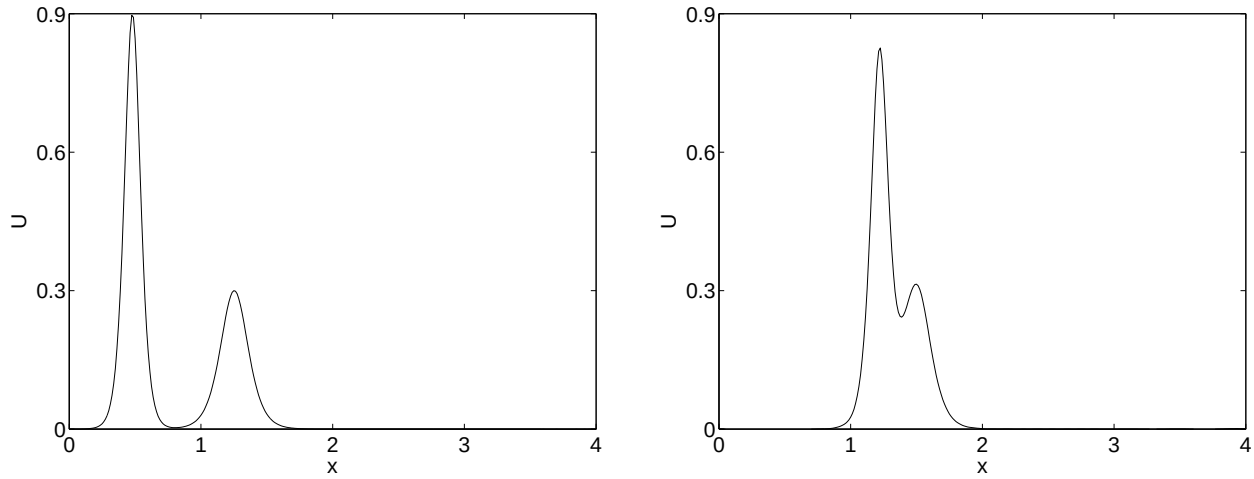

(a) (b)

Fig. 7: The plots of the two solitary waves obtained by the energy-preserving scheme: (a) $t = 0$, (b) $t = 2.5$, when $\alpha = 0$, $\beta = 1$, $\mu = 4.84 \times 10^{-4}$, $h = 0.0125$, $T = 6$, and $0 \leq x \leq 4$.

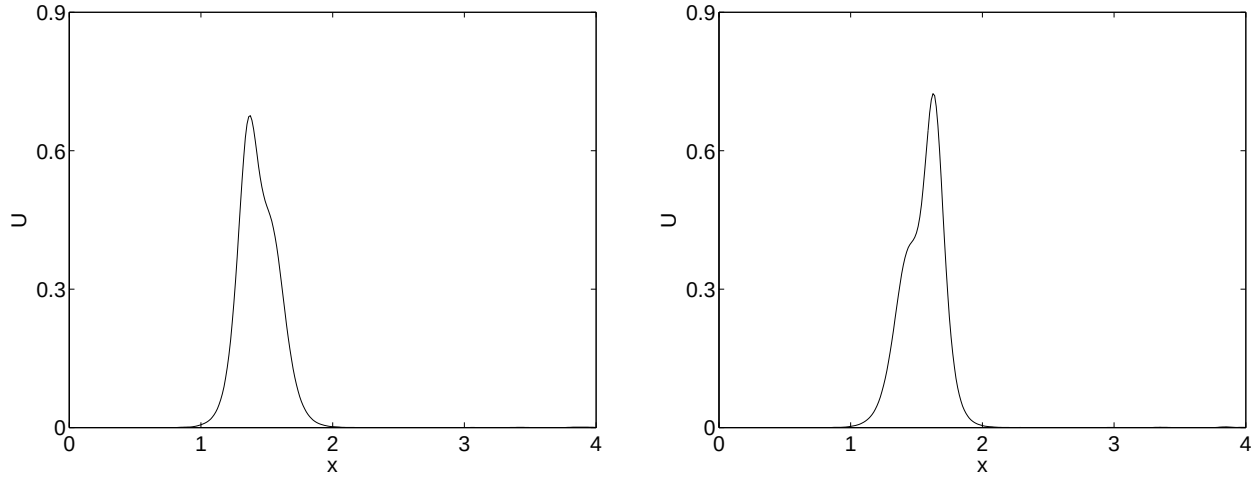

(c) (d)

Fig. 8: The plots of the two solitary waves obtained by the energy-preserving scheme: (c) $t = 3$, (d) $t = 3.5$, when $\alpha = 0$, $\beta = 1$, $\mu = 4.84 \times 10^{-4}$, $h = 0.0125$, $T = 6$, and $0 \leq x \leq 4$.

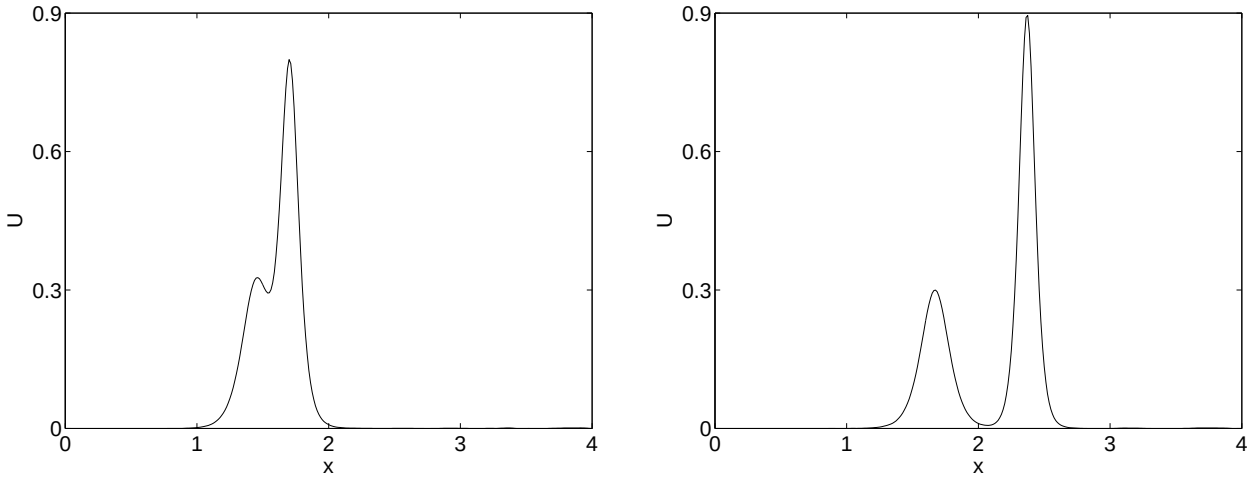

Fig. 9: The plots of the two solitary waves obtained by the energy-preserving scheme: (e) $t = 3.75$, (f) $t = 6$, when $\alpha = 0$, $\beta = 1$, $\mu = 4.84 \times 10^{-4}$, $h = 0.0125$, $T = 6$, and $0 \leq x \leq 4$.

REFERENCES

[1] D. J. Korteweg and G. de Vries, "On the change of form of long waves advancing in a rectangular channel and a new type of long stationary waves," *Philosophical Magazine*, vol. 39, no. 5, pp. 422–443, 1895.

[2] P. G. Drazin and R. S. Johnson, *Solitons: an Introduction*. Cambridge University Press, 1996.

[3] R. M. Miura, C. S. Gardner, and M. D. Kruskal, "Korteweg-de vries equation and Generalisation. II. Existence of Conservation Laws and Constants of Motion," *Journal of Mathematical Physics*, vol. 9, pp. 1204–1209, 1968.

[4] D. Furihata and T. Matsuo, *Discrete variational derivative method: a structure-preserving numerical method for partial differential equations*. CRC Press, 2010.

[5] D. Furihata and M. Mori, "A stable finite difference scheme for the Cahn-Hilliard equation based on a Lyapunov functional," *Journal of Applied Mathematics and Mechanics*, vol. 76, no. 1, pp. 405–406, 1996.

[6] S. Koide and D. Furihata, "Nonlinear and linear conservative finite difference schemes for regularized long wave equation," *Japan Journal of Industrial and Applied Mathematics*, vol. 26, no. 1, pp. 15–40, 2009.

[7] T. Matsuo and D. Furihata, "Dissipative or conservative finite difference schemes for complex-valued nonlinear partial differential equations," *Journal of Computational Physics*, vol. 171, no. 2, pp. 425–447, 2001.

[8] T. Yaguchi, T. Matsuo, and M. Sugihara, "An extension of the discrete variational method to nonuniform grids," *Journal of Computational Physics*, vol. 229, no. 11, pp. 4382–4423, 2010.

[9] T. Matsuo and H. Kuramae, "An alternating discrete variational derivative method," *AIP Conference Proceedings*, vol. 1479, no. 1, pp. 1260–1263, 2012.

[10] W. Hackbusch, "On first and second order box schemes," *Computing*, vol. 41, pp. 277–296, 1989.

[11] R. H. Li, Z. Y. Chen, and W. Wu, *Generalized Difference Methods for Differential Equations: Numerical Analysis of Finite Volume Methods*. Marcel Dekker, Inc., 2000.

[12] Q. X. Wang, Z. Y. Zhang, X. H. Zhang, and Q. Y. Zhu, "Energy-preserving finite volume element method for the improved Boussinesq equation," *Journal of Computational Physics*, vol. 270, pp. 58–69, 2014.

[13] Z. Y. Zhang, "Error estimates of finite volume element method for the pollution in groundwater flow," *Numerical Methods for Partial Differential Equations*, vol. 25, no. 2, pp. 259–274, 2009.

[14] J. L. Yan and Z. Y. Zhang, "Two-grid methods for characteristic finite volume element approximations of semi-linear Sobolev equations," *Engineering Letters*, vol. 23, no. 3, pp. 189–199, 2015.

[15] L. Z. Qian and H. P. Cai, "Two-grid method for characteristics finite volume element of nonlinear convection-dominated diffusion equations," *Engineering Letters*, vol. 24, no. 4, pp. 399–405, 2016.

[16] S. Li and L. Vu-Quoc, "Finite difference calculas invariant structure of a class of algorithms for the nonlinear Klein-Gordon equation," *SIAM Journal on Numerical Analysis*, vol. 32, no. 6, pp. 1839–1875, 1995.

[17] Z. Fei, V. M. Pérez-Garcia, and L. Vázquez, "Numerical simulation of nonlinear Schrödinger systems: a new conservative scheme," *Applied Mathematics and Computation*, vol. 71, no. 2-3, pp. 165–177, 1995.

[18] T. R. Taha and M. I. Ablowitz, "Analytical and numerical aspects of certain nonlinear evolution equations. III. Numerical, Korteweg-de Vries equation," *Journal of Mathematical Physics*, vol. 55, no. 2, pp. 231–253, 1984.

[19] S. Zhang and Z. Y. Wang, "Improved homogeneous balance method for multi-soliton solutions of Gardner equation with time-dependent coefficients," *IAENG International Journal of Applied Mathematics*, vol. 46, no. 4, pp. 592–599, 2016.

[20] U. M. Ascher and R. I. McLachlan, "Multisymplectic box schemes and the Korteweg-de Vries equation," *Applied Numerical Mathematics*, vol. 48, no. 3-4, pp. 255–269, 2004.

[21] D. D. Bhatta and M. I. Bhatti, "Numerical solution of KdV equation using modified Bernstein polynomials," *Applied Mathematics and Computation*, vol. 174, no. 2, pp. 1255–1268, 2006.

[22] M. T. Darvishi, S. Kheybari, and F. Khani, "A numerical solution of the Korteweg-de Vries equation by pseudospectral method using Darvishis preconditionings," *Applied Mathematics and Computation*, vol. 182, no. 1, pp. 98–105, 2006.

[23] I. Dağ and Y. Dereli, "Numerical solutions of KdV equation using radial basis functions," *Applied Mathematical Modelling*, vol. 32, no. 4, pp. 535–546, 2008.

[24] A. J. Khattak and U. I. Siraj, "A comparative study of numerical solutions of a class of KdV equation," *Applied Mathematics and Computation*, vol. 199, pp. 425–434, 2008.

Jin-liang Yan was born in Pingyao, Shanxi Province, china, in 1979. The author respectively received his Ph.D. and Master's degrees in computational mathematics at Nanjing Normal University, Nanjing, Jiangsu Province, China, in July 2016 and July 2010.

He holds a teaching position at Wuyi University, Information and Computation Science in the department of Mathematics and Computer. The Wuyi University is located in Wu Yi Shan, Fujian Province of China. His current research interests include structure-preserving algorithms, numerical solution of partial differential equations and computing sciences.

Liang-hong Zheng was born in Nanping, Fujian Province, China, in 1983. The author received her bachelor's degree in computer science and technology from Minnan Normal University, Zhangzhou, Fujian Province, China, in July 2009.

Also, she is a teacher at No. 1 Middle School in the department of Information and Technology. The No. 1 Middle School is located in Nanping, Fujian Province of China. Her current research interests include algorithm design, artificial intelligence, robot competition and video production.